

Article

Integrated microRNA–mRNA Expression Profiling Identifies Novel Targets and Networks Associated with Autism

Pritmohinder S. Gill ^{1,2,*}, Harsh Dweep ³, Shannon Rose ^{1,2}, Priyankara J. Wickramasinghe ³, Kanan K. Vyas ², Sandra McCullough ², Patricia A. Porter-Gill ², and Richard E. Frye ^{4,5}

¹ Department of Pediatrics, University of Arkansas for Medical Sciences, Little Rock, AR 72202, USA; srose@uams.edu

² Arkansas Children's Research Institute, Little Rock, AR 72202, USA; kkvyas@uams.edu (K.K.V.); mcculloughsandras@uams.edu (S.M.); portergillpa@archildrens.org (P.A.P.-G.)

³ The Wistar Institute, 3601 Spruce St., Philadelphia, PA 19104, USA; dweeph@gmail.com (H.D.); priyaw@wistar.org (P.J.W.)

⁴ Barrow Neurological Institute at Phoenix Children's Hospital, Phoenix, AZ 85016, USA; rrfrye@phoenixchildrens.com

⁵ Department of Child Health, University of Arizona College of Medicine, Phoenix, AZ 85004, USA

* Correspondence: psgill@uams.edu; Tel.: +1-501-364-2743

Abstract: Autism spectrum disorder (ASD) is a complex neurodevelopmental disorder, with mutations in hundreds of genes contributing to its risk. Herein, we studied lymphoblastoid cell lines (LCLs) from children diagnosed with autistic disorder ($n = 10$) and controls ($n = 7$) using RNA and miRNA sequencing profiles. The sequencing analysis identified 1700 genes and 102 miRNAs differentially expressed between the ASD and control LCLs ($p \leq 0.05$). The top upregulated genes were *GABRA4*, *AUTS2*, and *IL27*, and the top upregulated miRNAs were *hsa-miR-6813-3p*, *hsa-miR-221-5p*, and *hsa-miR-21-5p*. The RT-qPCR analysis confirmed the sequencing results for randomly selected candidates: *AUTS2*, *FMR1*, *PTEN*, *hsa-miR-15a-5p*, *hsa-miR-92a-3p*, and *hsa-miR-125b-5p*. The functional enrichment analysis showed pathways involved in ASD control proliferation of neuronal cells, cell death of immune cells, epilepsy or neurodevelopmental disorders, WNT and PTEN signaling, apoptosis, and cancer. The integration of mRNA and miRNA sequencing profiles by miRWalk2.0 identified correlated changes in miRNAs and their targets' expression. The integration analysis found significantly dysregulated miRNA–gene pairs in ASD. Overall, these findings suggest that mRNA and miRNA expression profiles in ASD are greatly altered in LCLs and reveal numerous miRNA–gene interactions that regulate critical pathways involved in the proliferation of neuronal cells, cell death of immune cells, and neuronal development.



Citation: Gill, P.S.; Dweep, H.; Rose, S.; Wickramasinghe, P.J.; Vyas, K.K.; McCullough, S.; Porter-Gill, P.A.; Frye, R.E. Integrated microRNA–mRNA Expression Profiling Identifies Novel Targets and Networks Associated with Autism. *J. Pers. Med.* **2022**, *12*, 920. <https://doi.org/10.3390/jpm12060920>

Academic Editor: Manuel Casanova

Received: 5 April 2022

Accepted: 27 May 2022

Published: 1 June 2022

Publisher's Note: MDPI stays neutral with regard to jurisdictional claims in published maps and institutional affiliations.



Copyright: © 2022 by the authors. Licensee MDPI, Basel, Switzerland. This article is an open access article distributed under the terms and conditions of the Creative Commons Attribution (CC BY) license (<https://creativecommons.org/licenses/by/4.0/>).

Keywords: autism spectrum disorder; lymphoblastoid cell lines; microRNA; mRNA; gene expression; RNA-seq; miRNA-seq

1. Introduction

Autism spectrum disorder (ASD) is an enigmatic neurodevelopment disorder that affects approximately 2% of children [1]. The etiology is not known in most cases, with studies suggesting that it involves multiple organs and physiological systems outside of the brain [2] and the deregulation of diverse subcellular molecular pathways [3]. For example, abnormalities in immune regulation; metabolism, including folate and energy metabolism; and redox regulations and methylation have been documented in multiple studies, but the origin of these abnormalities, how they are connected, and their effects on ASD symptoms remain unclear [4]. Molecular pathways including mTOR, PTEN, AKT, and β -catenin have also been found to be deregulated in ASD [3].

Lymphoblastoid cell lines (LCLs) provide a valuable tool to study underlying molecular regulation in ASD [5]. Biobanked LCLs have been utilized to study structural genetic

changes, such as copy number variations and gene mutations; changes in cellular regulation, including mRNA [6] and microRNA (miRNA) expression [7]; metabolic alteration, including alterations in mitochondrial function [8], redox [9,10], and methylation metabolism [11]; and changes in immune regulation [12].

MicroRNAs (miRNAs) are small non-coding RNAs with tissue-specific expression that regulate post-transcriptional gene expression [13]. Given the diverse pathways that have been found to be dysregulated in ASD, studying miRNA expression may be very promising, as miRNAs can regulate many seemingly unrelated molecular pathways and may result in diverse changes in gene expression depending on the tissue. Some initial studies have found alterations in miRNAs in ASD using LCLs [7,14,15]. Despite promising results, studies remain with inconsistent findings. Since miRNAs regulate mRNAs, one approach is to integrate analysis of changes in both mRNA and miRNA expression to explore regulatory networks.

This study presents the mRNA and miRNA sequencing profile of control and ASD LCLs and an integrative analysis of miRNA–mRNA expression using miRWalk 2.0. The findings from the bioinformatic analysis show that miRNAs potentially regulate mRNAs involved in the proliferation of neuronal cells, the cell death of immune cells, epilepsy or neurodevelopmental disorders, and the WNT/ β -catenin/PTEN signaling pathways.

2. Materials and Methods

Figure 1 shows the workflow of the investigation, showing the number of LCL samples used as controls and ASD groups and the steps for bioinformatic analysis of the sequencing data using miRWalk 2.0 and Ingenuity® Pathway Analysis software (IPA®).

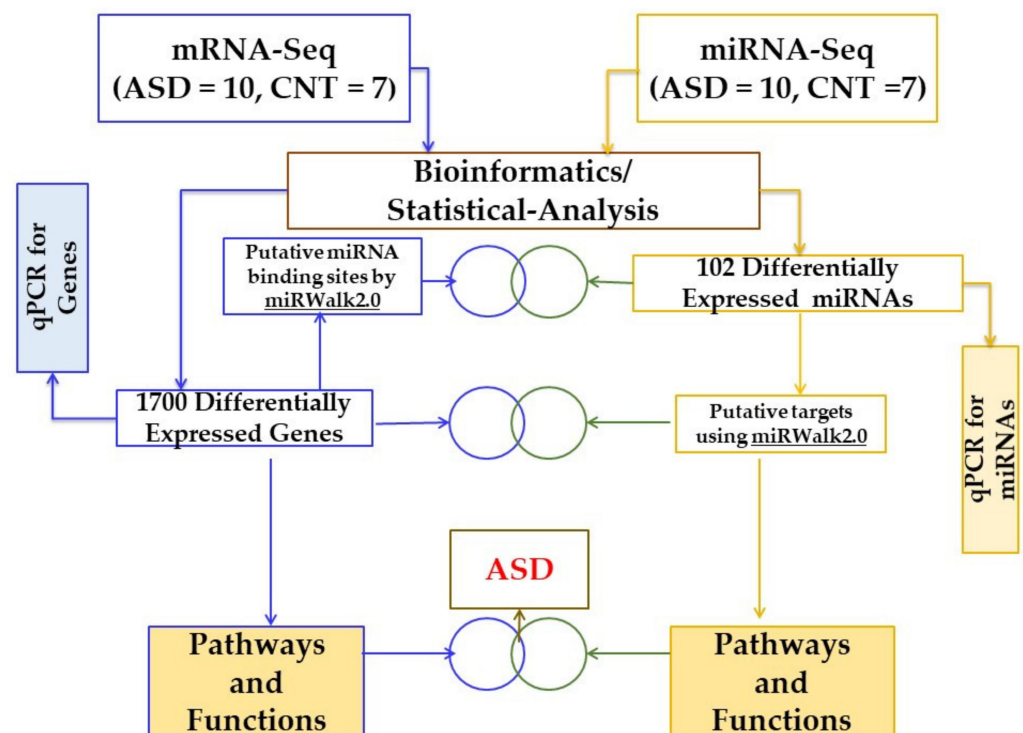


Figure 1. Schematic workflow to study differentially regulated genes, miRNAs, and pathways in ASD and CNT LCLs. ASD = autism, CNT = control, LCLs = lymphoblastoid cell lines.

2.1. Materials

The following materials were procured from various vendors: RPMI 1640 culture media, penicillin/streptomycin, fetal bovine serum (FBS), phosphate-buffered saline (PBS), and the BCA Protein Assay Kit were all obtained from Thermo Fisher Scientific (Waltham, MA, USA). For qRT-PCR reagents and vendors were the miRNeasy Mini Kit (Qiagen,

Valencia, CA, USA), RNeasy MinElute Cleanup Kit (Qiagen, Valencia, CA, USA), and miScript II RT kit (Qiagen, Valencia, CA, USA), SYBR green qRT-PCR assay (Qiagen, Valencia, CA, USA), and TaqMan assays (ThermoFisher Scientific, Carlsbad, CA, USA).

2.2. Cell Lines and Tissue Culture Conditions

Samples from children with autistic disorder were obtained from the Autism Genetics Resource Exchange (AGRE), a publicly available biomaterials repository located in Los Angeles, CA (AGRE; Los Angeles, CA, USA). AGRE collects samples from non-idiopathic cases of autism spectrum disorders. The procedures for screening children for collection are provided on the program website (<https://www.autismspeaks.org/agre-program>, accessed on 17 May 2022). Age and gender-matched controls with no documented behavioral or neurological disorder or a first-degree relative with a medical disorder were obtained from Coriell Cell Repository (Camden, NJ, USA).

LCLs were maintained in RPMI 1640 culture medium as previously described [7,8,10] in a humidified incubator at 37 °C with 5% CO₂. These LCLs were used in a previous study examining bioenergetics [10] and miRNA in ASD [7]. In this manuscript, LCLs from subjects with autistic disorder (ICD-9: 299.0; ICD-10: F84.0) are designated as ASD and those from controls are designated as CNT (Table 1).

Table 1. Lymphoblastoid Cell Lines (LCLs) used in this study from children with autistic disorder and age- and gender-matched control LCLs. Average age of each group is provided.

Unrelated Controls (CNT)		Study Sample Number (CNT)	Autism (ASD)		Study Sample Number (ASD)
ID	Age		ID	Age	
GM09621	8	09621C	03C14441	7	14441A-A
GM16007	12	16007C	03C16499	11	16499A-A
GM15862	11	15862C	AU0939303	11	2591A-A
GM11626	13	11626C	AU1165302	13	2746A-A
			AU1280302	7	3110A-A
			AU1393306	3	3540A-A
GM11599	9	11599C	AU1344302	7	3620A-A
GM09659	4	09659C	01C08495	4	8495A-A
			01C08594	7	8594A-A
GM10153	10	10153C	02C09713	10	9713A-A
Average (SD)	9.6 (3.0)			8.0 (3.2)	

2.3. RNA and Small RNA Sequencing

2.3.1. LCL RNA Sequencing (RNA-Seq)

Total RNA was extracted using Trizol reagent (ThermoFisher, Carlsbad, CA, USA) following the manufacturer’s procedure. The total RNA quantity and purity were analyzed by the Bioanalyzer 2100 and RNA 6000 Nano LabChip Kit (Agilent, Santa Clara, CA, USA) with an RIN number of >7.0. Approximately 10 ug of total RNA was subjected to isolated Poly (A) mRNA with poly-T oligo attached magnetic beads (ThermoFisher, Carlsbad, CA, USA). Following purification, the poly(A)- or poly(A)+ RNA fractions were fragmented into small pieces using divalent cations under an elevated temperature. The cleaved RNA fragments were reverse transcribed to create the final cDNA library in accordance with the protocol for the mRNA-seq sample preparation kit (Illumina, San Diego, CA, USA) and the average insert size for the paired-end libraries was 300 bp (±50 bp). Finally, paired-end sequencing was performed on an Illumina Hiseq 4000 following the vendor’s recommended protocol.

2.3.2. LCLs Small RNA Sequencing (miRNA-Seq)

Total RNA was extracted using Trizol reagent (ThermoFisher, Carlsbad, CA, USA) following the manufacturer's procedure. The total RNA quantity and purity were assessed with Bioanalyzer 2100 (Agilent, Santa Clara, CA, USA) with an RIN number of >7.0. Small RNA enrichment was performed by the excision of the 15 to 50 nt fraction from a polyacrylamide gel. Approximately 1 µg of enriched RNA was used to prepare the small RNA library, according to the protocol of the TruSeq Small RNA Sample Prep Kits (Illumina, San Diego, CA, USA). Finally, single-end sequencing (36 bp or 50 bp) was performed on an Illumina HiSeq 2500 at LC Sciences (Houston, TX, USA) following the vendor's recommended protocol.

2.4. Bioinformatics Analysis for RNA-Seq

The raw reads of both sequencing profiles were aligned using Bowtie [16] against the hg19 version of the human genome, and RSEM v1.2.12 software [17] was used to estimate raw read counts using Ensemble v84 gene information. DESeq2 [18] was utilized to identify differentially expressed genes between sample groups. Samples with poor alignment rates were identified as outliers in quality control analysis and therefore removed before carrying out the differential expression analysis. A false-positive rate of $\alpha = 0.05$ with false-discovery rate (FDR) correction was used as the level of significance. Only a handful of genes were found to satisfy the FDR < 5% cut-off, which was not sufficient for functional enrichment analysis. Therefore, it was decided to consider a $p < 0.05$ threshold to select differentially expressed genes. These genes were then subjected to functional enrichment analysis.

2.5. Functional Annotation of Differentially Expressed Genes

Pathway and functional enrichment analyses were tested on genes that passed a significant p -value of <0.05 using QIAGEN's Ingenuity® Pathway Analysis (IPA®, QIAGEN Redwood City, CA, USA) software. The most relevant ($p < 0.05$) pathways and functions associated with autism were selected to generate dot plots using a customized R script.

2.6. miRNA Target Predictions using miRWalk2.0

The miRWalk2.0 database was used to gather putative miRNA binding sites within the DEGs [19,20]. miRWalk3.0 is a new publicly available version of miRWalk2.0. However, miRWalk3.0 is not very useful for carrying out miRNA-target predictions, as it fails to offer users the flexibility to choose the prediction algorithm of their choice, and at the same time, it entirely misses all the key features that are of utmost importance to the scientific community (e.g., a meta-analysis of targets by 13 different prediction datasets). On the other hand, the miRWalk2.0 database offers a meta-analysis of putative miRNA binding sites by collecting 13 prediction datasets from existing miRNA-target resources, which can help reduce the number of false-positive targets [21,22].

2.7. Integrated Analysis of RNA- and miRNA-Sequencing Data

After the initial analysis of removing bad quality reads, the DESeq2 package [18] was utilized to normalize the raw counts and fit models to identify differentially expressed genes (DEGs) and miRNAs (DEMs) between ASD and control samples. The level of significance was set to $p < 0.05$. The meta-analysis platform of the miRWalk2.0 database [19,21] was employed for this integrated analysis to collect putative interactions between significant genes and miRNAs. The interactions among significant genes and miRNAs predicted with at least 2 algorithms were compiled into a list (only DEGs) and were uploaded to IPA for enrichment analysis and identification of associated networks (Figure 1).

2.8. Quantitative Reverse-Transcriptase-Polymerase Chain Reaction (qRT-PCR) Validation

LCLs were used to isolate total RNA and microRNA as previously described [7]. Briefly, RNA isolated with miRNeasy Mini Kit (Qiagen, Valencia, CA, USA) and miRNA isolated with RNeasy MinElute Cleanup Kit (Qiagen, Valencia, CA, USA) were used to

perform cDNA synthesis with the miScript II RT kit (Qiagen, Valencia, CA, USA). The qRT-PCR was run in triplicate on a QuantStudio™ 6 Flex Real-Time PCR System (ThermoFisher Scientific, Carlsbad, CA, USA).

Supplementary Table S1 shows the assay ID and catalog number for the TaqMan gene expression assay (ThermoFisher Scientific, Inc., Carlsbad, CA, USA) for *AUTS2*, *FMR1*, and *PTEN*. SYBR green miScript assays (Qiagen, Valencia, CA, USA) for miRNA expression were used for *Hsa-miR-15a-5p*, *Hsa-miR-92a-3p*, and *Hsa-miR-125b-5p* (Supplementary Table S2). Taqman assays were duplexed with *GAPDH* to normalize the mRNA expression. miRNA data normalization was conducted with an exogenous control (Ce-miR-39) and an endogenous control (*RNU6*).

Negative controls and no template controls (NTC) were run with each assay. Relative quantitation for miRNA and mRNA was calculated using the $2^{-\Delta\Delta Ct}$ method.

2.9. Statistical Analysis

All experimental data for qRT-PCR are presented as means ± SEM, and differences between the two groups were examined using Student's *t*-test (2-tailed). *p*-Values of less than 0.05 were considered significant.

3. Results

3.1. Identification of Differentially Expressed Genes and miRNAs

The top candidate genes and miRNAs are shown in Figures 2 and 3. The samples with poor alignment rates were dropped from the subsequent analysis. These results demonstrated that genes and miRNAs were differentially expressed between ASD and control samples. A false-positive rate of $\alpha = 0.05$ with false discovery rate (FDR) correction was used as the level of significance.

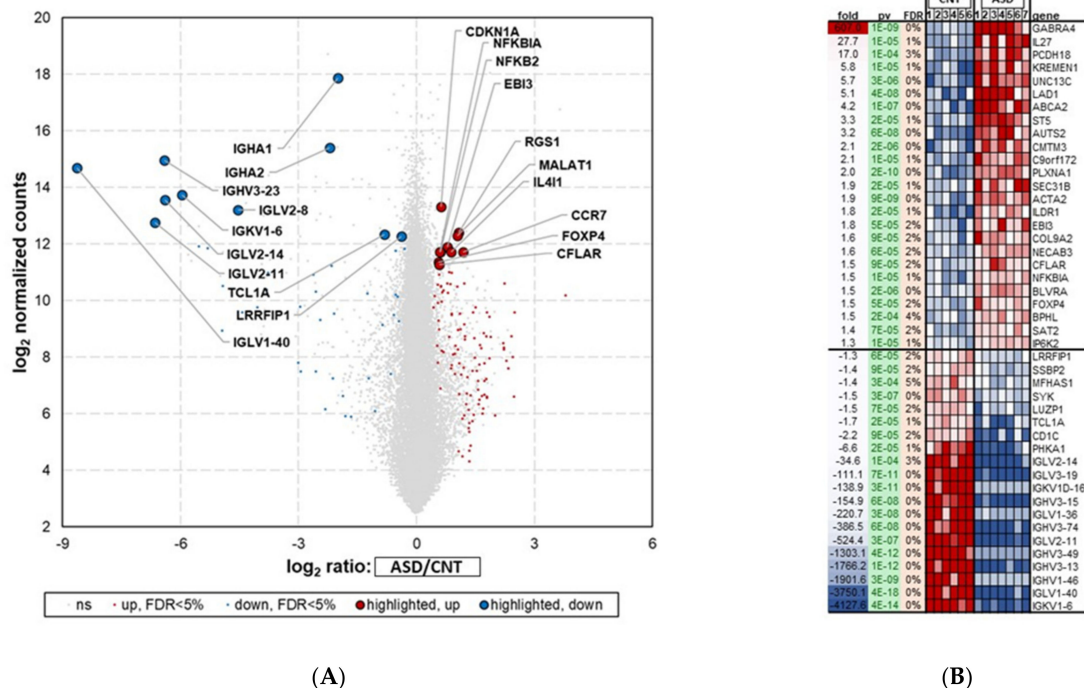


Figure 2. RNA-seq analysis showing differential expression of top 45 mRNAs in LCL groups—ASD (*n* = 7) and CNT (*n* = 6)—with FDR < 5%. Samples with poor alignment rates which were dropped from differential expression analysis, included 3 from ASD group and one from Control group. (A) Volcano plot of differentially expressed mRNAs (DEGs) in ASD and CNT LCLs. (B) Heatmap of DEGs in ASD and CNT LCLs. ASD = Autism, CNT = Control, Fold = Fold Change, *pv* = *p*-value and gene symbol. Red dots are upregulated, blue dots are downregulated, and grey dots indicate no change; FDR = false discovery rate.

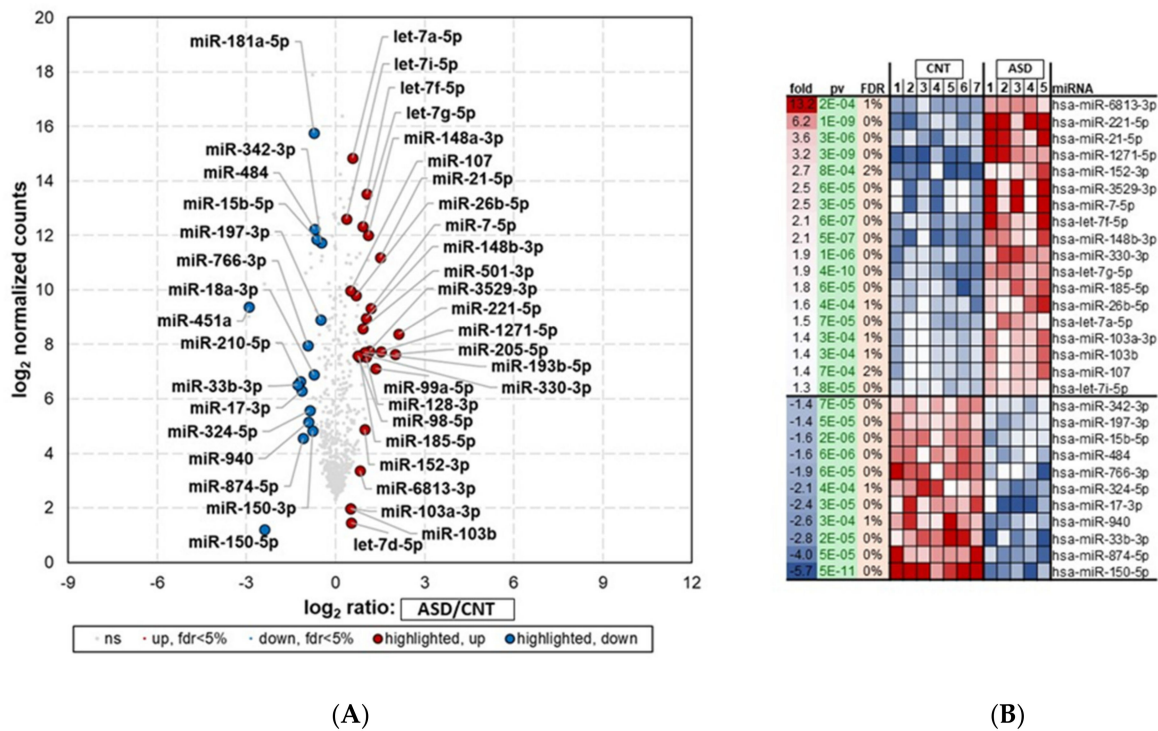


Figure 3. miRNA-seq analysis showing differential expression of top 29 miRNAs in LCLs groups—ASD ($n = 5$) and CNT ($n = 7$)—with FDR < 5%. Samples with poor alignment rates which were dropped from differential expression analysis, included 5 from ASD group. (A) Volcano plot of differentially expressed miRNAs in ASD and CNT LCLs. (B) Heatmap of differentially expressed miRNAs in ASD and CNT LCLs. ASD = Autism, CNT = Control, Fold = Fold change, pv = p -value, and miRNA. Red dots are upregulated, blue dots are downregulated, and grey dots indicate no change; FDR = false discovery rate.

3.1.1. Differential Gene Expression in ASD LCLs

The RNA-seq analysis showed 1700 significantly ($p < 0.05$) differentially expressed mRNAs (DEGs) between the ASD and control groups (Figure 2A). The list of deregulated genes shows that 629 were downregulated and 1071 were upregulated (Table S3).

The top 45 (25 most upregulated and 20 most downregulated) differentially regulated genes (FDR < 5%) in ASD LCLs compared with control LCLs are depicted in Figure 2B. ASD LCLs showed highly upregulated expression for *GABRA4*, with a fold change of 607 ($p < 0.05$), followed by *IL27*, with a fold change of 27.7 ($p < 0.05$), compared with control LCLs. By contrast, the downregulated genes ($p < 0.05$) were from immunoglobulin light chain and heavy chain members in ASD LCLs, e.g., *IGKV1-6*, with a fold change of -4127.6, followed by *IGLV1-40*, with a fold change of -3750 ($p < 0.05$).

3.1.2. Differentially Expressed miRNAs in ASD LCLs

The small RNA-seq analysis (miRNA-seq) showed 102 differentially expressed miRNAs (DEMs) in ASD compared with control samples ($p < 0.05$) (Figure 3A; Supplementary Table S4). Of these, 37 miRNAs were downregulated, and 65 were upregulated.

The top 29 (18 most upregulated and 11 most downregulated) differentially regulated miRNAs (FDR < 5%) in ASD LCLs compared with control LCLs are depicted in Figure 3B. ASD LCLs showed significant upregulation for a number of miRNAs ($p < 0.05$) compared with control LCLs. These included *hsa-miR-6813-3p*, *hsa-miR-221-5p*, and *hsa-miR-21-5p*, with fold changes of 13, 6.2, and 3.6, respectively. The top downregulated miRNAs ($p < 0.05$) were *hsa-miR-150-5p*, *hsa-miR-874-5p*, and *miR-15b-5p*, with fold changes of -5.7, -4, and -1.6, respectively.

3.2. qRT-PCR Validation of Differentially Expressed miRNAs and Genes

To verify the findings of both sequencing results, we randomly selected three differentially expressed genes and three differentially expressed miRNAs for qRT-PCR validation.

3.2.1. Gene Expression Validation by qRT-PCR

To validate the RNA-seq dataset, the expression levels of the three randomly selected genes *AUTS2*, *FMR1*, and *PTEN* were determined by qRT-PCR analysis. The expression levels of *AUTS2* (Figure 4A) were upregulated 3.7-fold in ASD LCLs compared with the control LCLs ($p \leq 0.05$). The other two mRNAs, *FMR1* (Figure 4B) and *PTEN* (Figure 4C), were significantly downregulated in ASD LCLs compared with the control LCLs ($p \leq 0.05$).

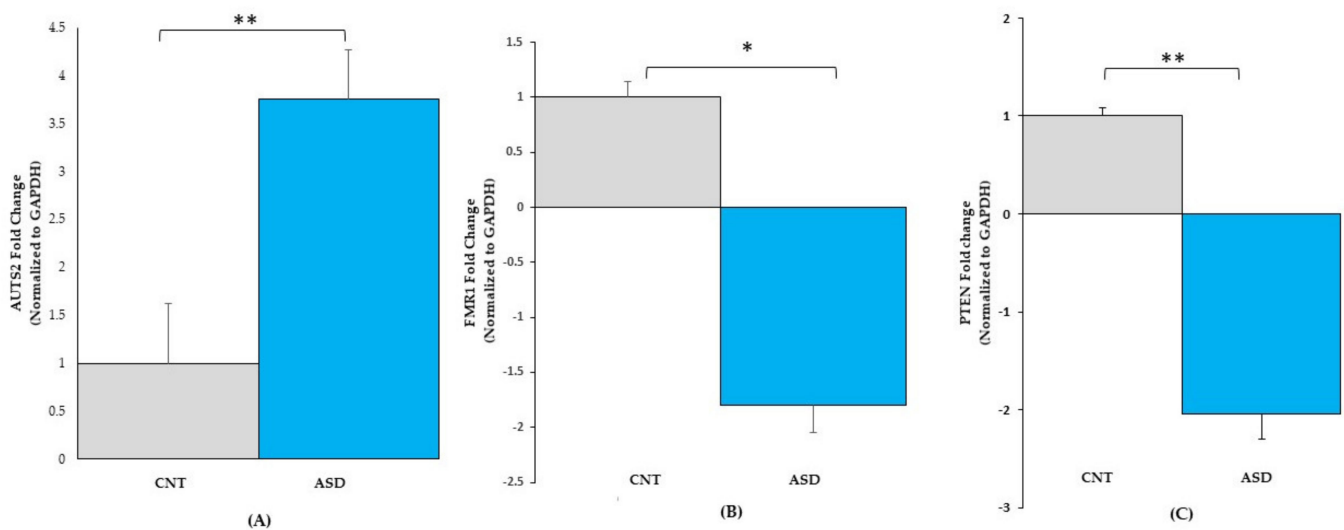


Figure 4. qRT-PCR validation of gene expression in LCL groups for (A) *AUTS2*: CNT ($n = 4$), ASD ($n = 4$), (B) *FMR1*: CNT ($n = 7$), ASD ($n = 10$) and (C) *PTEN*: CNT ($n = 7$), ASD ($n = 10$). ASD = Autism, CNT = Control, * = $p < 0.05$, ** = $p < 0.0001$; error bars represent standard error of the mean.

3.2.2. miRNA Expression Validation by qRT-PCR

To validate the miRNA-seq dataset, the three miRNAs, *hsa-miR-15a-5p*, *hsa-miR-92a-3p*, and *hsa-miR-125b-5p* (Figure 3 and Table S2), were randomly chosen for qRT-PCR analysis. The expression levels of *miR-15a-5p* (Figure 5A) were downregulated 2.2-fold in ASD LCLs compared with the control LCLs ($p \leq 0.05$). The other miRNA *miR-92a-3p* (Figure 5B) was also significantly downregulated in ASD LCLs compared with the control LCLs ($p \leq 0.05$). By contrast, *miR-125b-5p* (Figure 5C) was significantly upregulated in ASD LCLs compared with the control LCLs ($p \leq 0.05$). These results confirm the miRNA-seq dataset for the differentially expressed miRNAs in ASD LCLs.

3.3. Pathway Analysis of Differentially Expressed Genes

A total of 1700 DEGs and 102 DEMs with $p < 0.05$ were selected to test for pathway enrichment analysis using IPA software. The significantly expressed genes can participate in a network of diverse signaling pathways, such as apoptosis, cell death of immune cells, cell cycle progression, epilepsy, nNOS, and proliferation of neuronal cells (Figure 6). Z-scores are represented by red or blue colors for the signaling pathways. The activated pathways (shown in red) were related to cell death of immune cells, inflammatory response, the proliferation of neuronal cells, central nervous system solid tumor, epilepsy, the endocannabinoid neuronal synapse pathway, and synaptic long-term potentiation. Inhibited pathways (shown in blue) controlled apoptosis, inflammation of the organs, movement disorders, motor dysfunction, PI3K/AKT, ATM, and PTEN (Supplementary Tables S5 and S6).

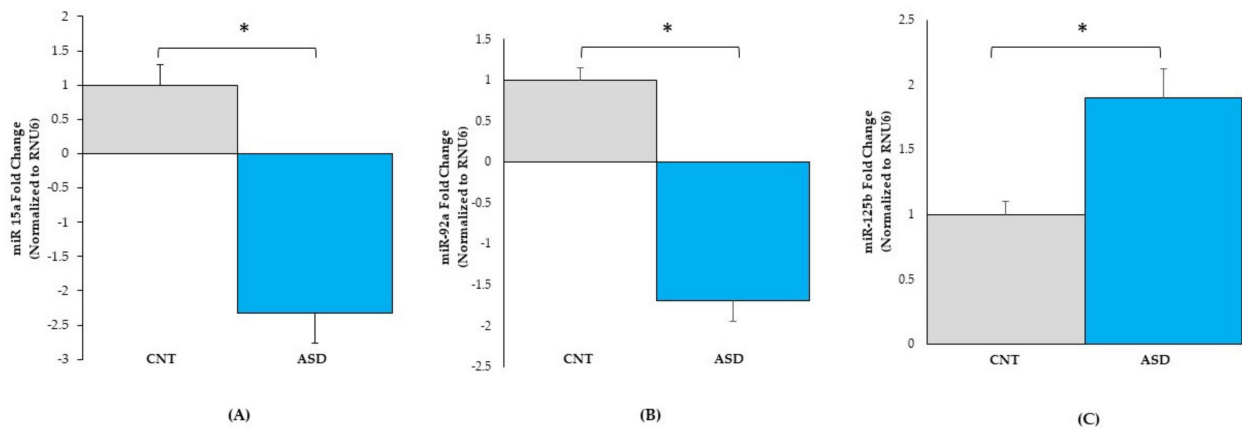


Figure 5. qRT-PCR validation of miRNA expression in control ($n = 7$) and ASD ($n = 10$) LCLs. *miR-15a-5p* (A), *miR-92a-3p* (B), and *miR-125b-5p* (C). ASD = autism, CNT = control; * = $p < 0.05$ compared to controls; error bars represent standard error of the mean.

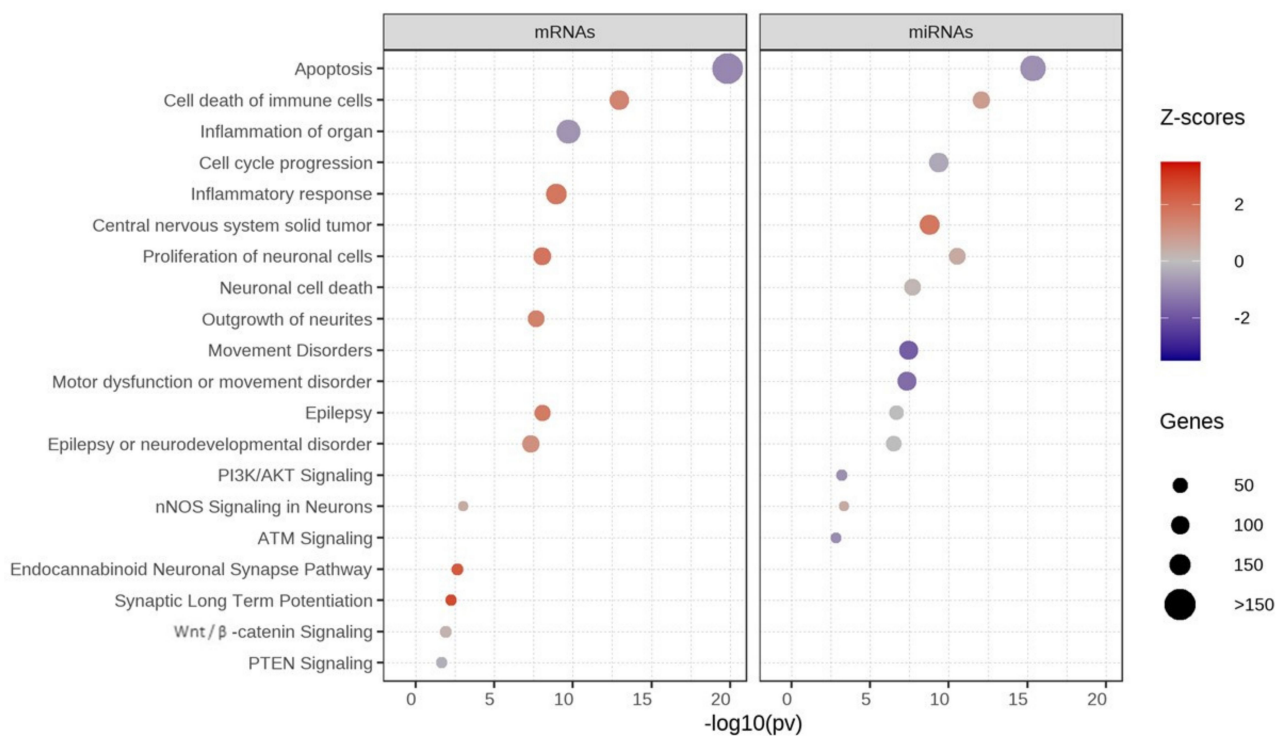


Figure 6. Pathway enrichment analysis of significant mRNAs and miRNAs-Ingenuity Pathway Analysis (IPA). Z-scores show activation or inhibition of pathways associated with autism. Red = activated pathway, blue = inhibited pathway, size of circle = number of genes.

3.4. Functional Enrichment Analysis of Differentially Expressed Genes

Subsequently, the 1700 DEGs and 102 DEMs ($p < 0.05$) were further selected to test for functional enrichment analysis using IPA software. Interestingly, these genes are also associated with diverse functions related to cancer, apoptosis, cellular homeostasis, movement disorders, and proliferation of neuronal cells (Figure 7). The genes with activated functions (shown in red) regulate cancer, cell survival, cell death of immune cells, neuronal cell death, the endocannabinoid neuronal synapse pathway, and synaptic long-term potentiation. By contrast, genes with inhibited functions (shown in blue) were involved in apoptosis, movement disorders, motor dysfunction, seizure, colon cancer, ATM signaling, PI3K/AKT signaling, and neuronal cell death. For details on various functions associated with ASD and control LCLs, see Supplementary Tables S5 and S6.

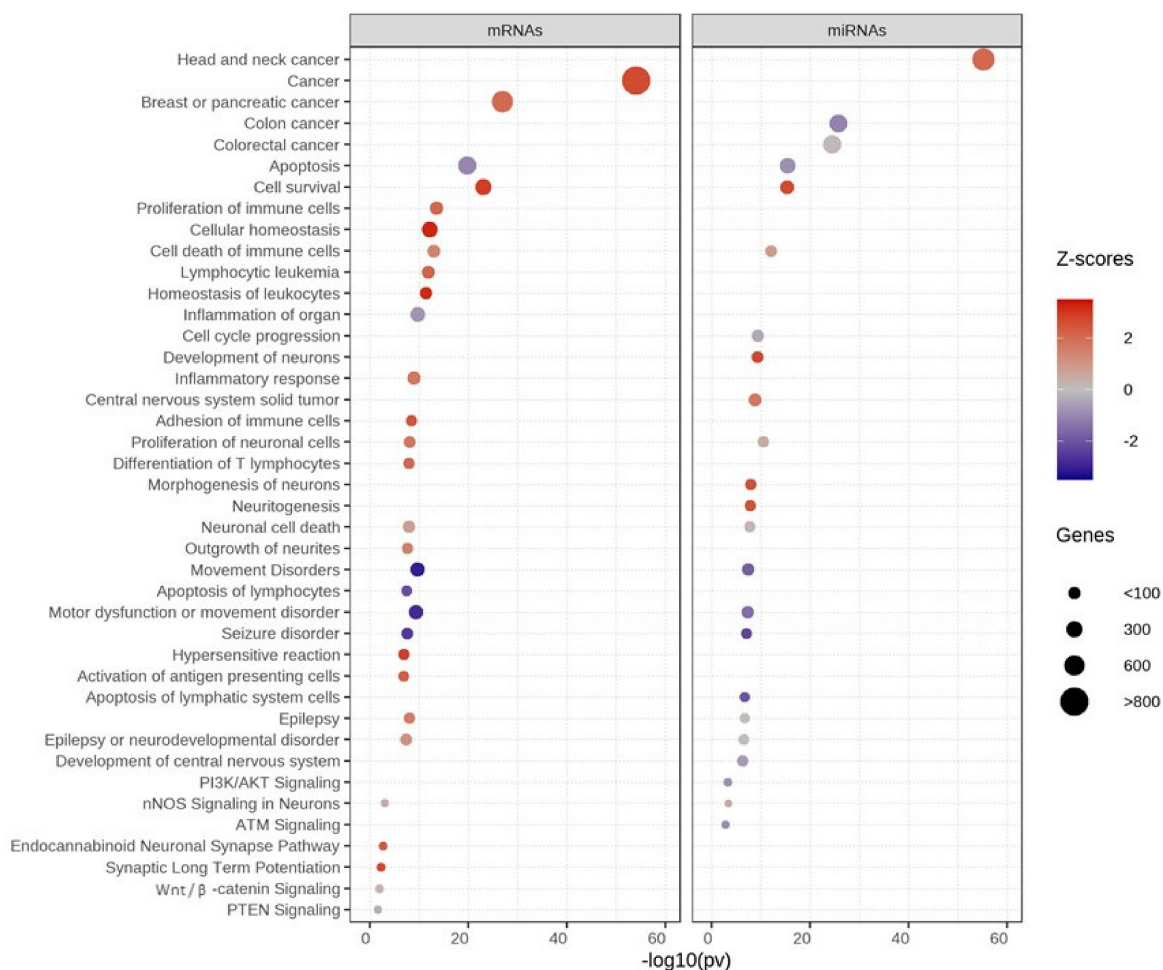


Figure 7. Functional enrichment analysis of significant mRNAs and miRNAs using IPA. Z-scores show functional enrichment. Red = activated, blue = inhibited, size of circle = number of genes.

3.5. Integrated Analysis of miRNA and mRNA Expression

The mRNA–miRNA interaction analysis using miRWalk2.0 showed 267 genes in significant pathways that were predicted to be targeted by deregulated miRNAs (Supplementary Table S7). These pathways control cell death of immune cells, the proliferation of neuronal cells, epilepsy or neurodevelopmental disorders, and Wnt/ β -catenin and PTEN signaling (Table S7). The activated pathways are shown in red, whereas the inhibited pathways are shown in blue.

The ASD LCLs showed upregulation of *GABRA4*, *IL27*, and *PTEN*; the downregulated genes were *FOXP1*, *NTN1*, and *NCAM2* (Figure 8 and Table S7). For example, *GABRA4* was upregulated 606-fold in ASD LCLs and regulated pathways of epilepsy and neurodevelopmental disorders (Figure 8, Table S7). *GABRA4* was predicted to be targeted by 16 upregulated miRNAs and 10 downregulated miRNAs (Figure 8, Table S7). By contrast, only *miR-3529-3p* (Table S7) was validated to be the target of *GABRA4*. Table S7 also shows that *miR-3529-3p* was upregulated twofold (red) in ASD LCLs, and this has been validated by two publications. *PTEN* regulates pathways of cell death of immune cells and proliferation of neuronal cells. *PTEN* was targeted by *miR-21-5p*, which was upregulated fourfold in ASD LCLs, and this has been validated by 62 publications (Table S7). *miR-3529-3p* also targets *NCAM2*, which was upregulated 6.06-fold (Figure 8). The sequencing results showed that *miR-3529-3p* was upregulated twofold in ASD LCLs, and only one publication validates this result (Table S7).

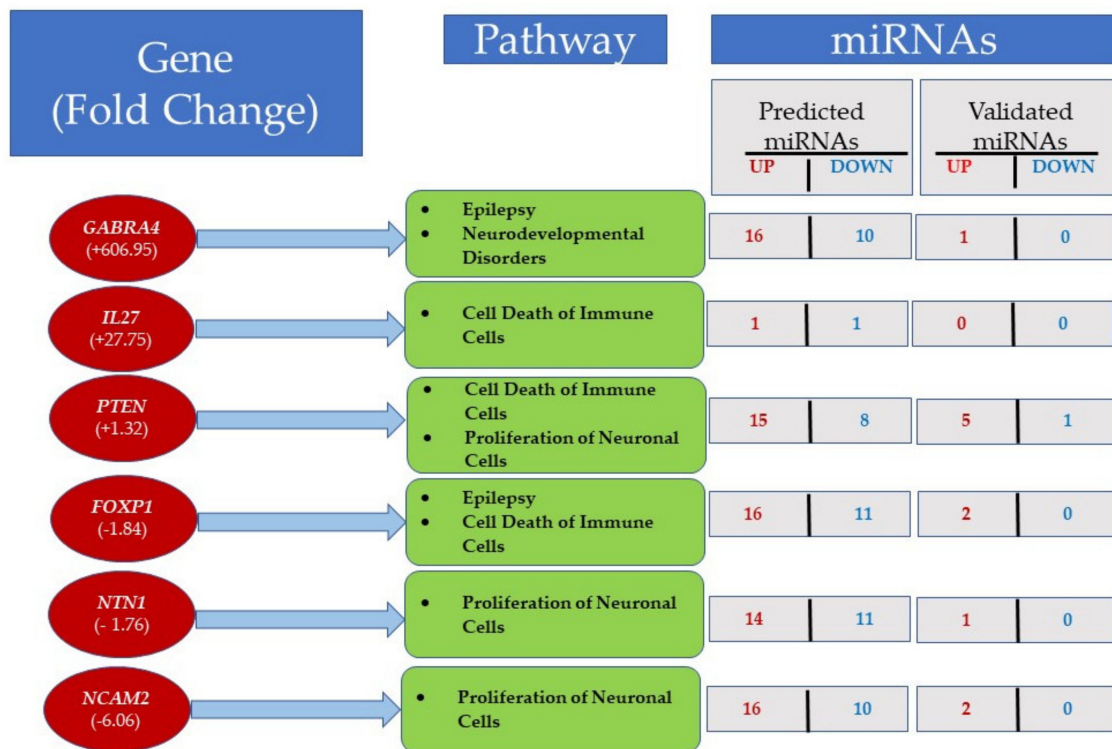


Figure 8. mRNA–miRNA interactions were predicted using differentially expressed genes targeted by miRNAs with miRWalk2.0. The figure shows some important pathways in LCLs, along with the number of predicted and validated miRNAs. For details see Table S7.

ASD LCLs show the pathways of cell death of immune cells are also activated by *IL27*, *PTEN*, and *FOXP1* (Figure 8), whereas *PTEN*, *NTN1*, and *NCAM2* regulate the pathway of the proliferation of neuronal cells.

4. Discussion

The RNA-seq analysis in our study showed 1700 DEGs in ASD LCLs compared with control LCLs. Most notably, *GABRA4*, *KREMEN1*, *PLXNA1* and *IL27* were elevated in ASD LCLs compared with control LCLs, whereas the majority of significantly downregulated genes were from immunoglobulin family members (*IGLV1-40*, *IGKV1-6*, and *IGHV3-13*) (Figure 2). Of the 102 DEMs, this study revealed that numerous miRNAs, notably *miR-6813-3p*, *miR-221-5p*, *miR-3529-3p*, *miR-1271-5p* and *miR-21-5p* were upregulated, whereas *miR-150-5p*, *miR-874-5p*, *miR-940*, *miR-17-3* and *miR-33b-3p* were markedly downregulated (Figure 3) in the ASD LCLs compared with control LCLs.

4.1. Dysregulated Expression at Transcriptomic and Epigenetic Levels in ASD

Previous transcriptomic [6,14,15,23–28] and epigenetic [14,15,23] studies on LCLs in ASD help us understand the genes and their functional pathways involved in the risk of developing ASD. For example, Talebizadeh et al. 2014 [24] looked at alternate splicing in ASD using LCLs and identified *CYFIP1*, *ZMYM6*, and *TRAP150* as potential ASD candidate genes. The RNA-seq dataset from the current study could not detect *TRAP150* and showed no significant change for *CYFIP1* and *ZMYM6*. Hu and colleagues [25] showed that the *NFKB1* and *MBD2* to be a strong candidate for genes for ASD, and the RNA-seq data on ASD LCLs did not detect expression of *MBD2* or *NFKB1*. Mutations in the fragile X mental retardation 1 gene (*FMR1*) are associated with the inherited form of ASD, and Nishimura and colleagues [26] found downregulation of *FMR1* in ASD vs. control samples, and our study confirmed this with qRT-PCR ($p < 0.05$) (Table S3 and Figure 5). However, for the

JAKMIP1 and *GPR155* genes, which were differentially expressed in their study [26], our RNA-Seq ASD LCLs data show no significant change for *JAKMIP1* and *GPR15* (Table S3).

Significant expression of *HEY1*, *SOX9*, *miR-486-3p/5p*, and *miR-181c* was observed in ASD LCLs [23], but our current RNA-seq dataset results did not reach significant level for these genes. *MiR-146* was upregulated in ASD LCLs [15], and the current miRNA-seq dataset confirmed the significant upregulation of *miR-146b-5p* (FC = 1.99; $p = 0.006$) (Table S3). Another study on ASD LCLs [14] reported upregulation of *miR-29b* and downregulation of *miR-199b*. The miRNA-seq data showed upregulation of *miR-199b-5p* and *miR-199b-3p* with no significant p -value, whereas *miR-199a-5p* showed significant upregulation in ASD LCLs (FC = 5.8, $p = 0.0065$). For *miR-29b*, our data showed downregulation, but the results did not reach statistical significance.

ASD LCLs showed significant upregulation of *GABRA4* (Figure 2). An association involving *GABRA4* has been reported in ASD patients [27,28], and this is the major inhibitory neurotransmitter in the mammalian brain. *GABRA4* is expressed in the thalamus, striatum, cerebral cortex, dentate gyrus (DG), and CA1 region of the hippocampus [29]. Another well-known gene in autism is *AUTS2*, and this study reported upregulation of *AUTS2* expression in ASD LCLs compared with control LCLs (Figure 2, Figure 4A). Most studies have reported intragenic de novo deletions of *AUTS2* [30–32] and have rarely described disease point mutations [33].

Many studies using LCLs as model cell type to understand autism, including this one, have many limitations, particularly the modest sample sizes in the context of the heterogeneous nature of ASD. Indeed, ASD is defined by a collection of various symptoms, which can be different from patient to patient. Although some categories are used as modifiers of the diagnosis, such as with and without language impairment or intellectual disability, the variation in symptoms has been difficult to easily describe or categorize. Thus, without well-defined subgroups, it may be difficult to find consistency with modest sample sizes. Clearly, larger studies on well-defined groups of individuals with ASD will be needed in the future. However, despite the heterogeneous nature of ASD, this study was consistent with some previous studies.

4.2. Immune Abnormalities and ASD

Immunoglobulin polymorphisms are known for infection and auto-immune disease susceptibility. Dysfunction of the immune system appears to be associated with ASD. A recent meta-analysis demonstrated evidence for immunological dysregulation in ASD with a reduction in total IgG and an elevation in the IgG4 subset [34]. In addition, studies have demonstrated that total IgM and IgG concentrations correlate with aberrant behavior with lower immunoglobulin concentrations being associated with worse behavior [35]. Additionally, a meta-analysis also demonstrated that intravenous immunoglobulin improved aberrant behavior, specifically irritability, hyperactivity, and social withdrawal [34]. Thus, this clinical data is consistent with the findings of decreased expression of genes involved in the production of IgG.

IL-27 is a pleiotropic cytokine involved in infection, cellular stress, neurological disease, and cancer that has complex activating and inhibitory properties in both innate and acquired immunity [36]. It is secreted from and binds to microglia, macrophages, and neurons and promotes neuronal survival by regulating cytokines, neuroinflammation, oxidative stress, apoptosis, autophagy, and epigenetics [36].

IL-27 gene expression was found to be markedly elevated in ASD LCLs. In the BTBR mouse model of ASD, studies have demonstrated that IL-27 agonist normalized neuroimmune dysfunction [37] yet other studies show that methylmercury [38] and tyrosine kinase inhibitor tyrphostin AG126 [39] decrease IL-27 in the BTBR mouse model. Another study demonstrated decreased IL-27 production by CD14+ cells derived from ASD individuals following in-vitro immunological challenge [40].

4.3. Integrated Analysis of ASD-CNT LCLs

Following, RNA-Seq and functional enrichment, an integrated analysis recognized a series of potential miRNA-mRNA interactions with implications in regulation of diverse networks. For example, *PTEN* was shown to be downregulated by RNA-seq analysis (Table S3) and RT-qPCR (Figure 4C). *PTEN* silencing enhances neuronal proliferation and differentiation by activating the PI3K/Akt/GSK3 β pathway [41]. *PTEN* regulates the pathways for cell death of immune cells and the proliferation of neuronal cells (shown in red). Table S7 also shows that *PTEN* was predicted to be targeted by 15 upregulated miRNAs, such as *miR-221-5p*, *miR-21-5p*, *miR-148b-3p*, and *miR-26b-5p*, and there were five validated targets: *miR-21-5p*, *miR-152-3p*, *miR-26b-5p*, *miR-103a-3p*, and *miR-107*. For example, *miR-21-5p* was upregulated in ASD LCLs fourfold (Table S7). *GABRA4* showed a 606.95-fold upregulation in ASD LCLs (Figure 2, Table S7) and is a target for *miR-3529-3p*. A role of *GABRA4* has been shown in ASD and seizure susceptibility [42,43]. The integrated analysis showed that it regulates the pathway for epilepsy or neurodevelopmental disorders; it is predicted to be targeted by 10 miRNAs: *miR-150-5p*, *miR-874-5p*, *miR-33b-3p*, *miR-940*, *miR-17-3p*, *miR-324-5p*, *miR-766-3p*, *miR-484*, *miR-197-3p*, and *miR-342-3p*. Similarly, the upregulated gene *IL27* (Figure 2, Table S3) plays an important neuroprotective role [25], and the integrated analysis showed that it is important in cell death of immune cells, has one predicted target (*miR-7-5p*), and has no validated miRNA. Multiple studies have converged on the dysregulation of the Wnt/ β -Catenin pathway in association with ASD [44], including studies using mouse [45], *Drosophila*, and zebrafish [46] animal models and patient cases [47].

The integrated analysis of miRNA-mRNA showed that 29 miRNAs (18 upregulated and 11 downregulated) and 267 genes formed miRNA-target gene pairs, which may have a role in complex network to regulate the proliferation of neuronal cells, cell death of immune cells, epilepsy or neurodevelopmental disorders, and Wnt/ β -catenin and *PTEN* signaling (Figure 8). Table S7 represents new mediators of abnormal gene expression that could be potential targets for further exploration and therapeutic interventions in the proliferation of neuronal cells, epilepsy or neurodevelopmental disorders, and Wnt/ β -catenin and *PTEN* signaling. However, functional validation is needed to test our miRNA-mRNA integration findings in ASD LCLs.

4.4. Autism and Cancer Genes Link?

Some have observed an overlap between the molecular pathways in ASD and cancer [48]. In this study, we found many cancer genes that demonstrated changes in both mRNA and miRNA expression in the ASD LCLs. The ASD LCLs demonstrated the downregulation of mRNA of several tumor suppressor genes, including *KREMEN1* [49], *ST5* [50], *ILDR1* [51], and *FOXP4* [52].

The ASD LCLs demonstrated upregulation of several oncogenes, including *SYK* [53–55], *MFHAS1* [56–59], and *TCL1A* [60]. Interestingly, *MFHAS1* has also been implicated in sepsis-associated encephalopathy [61] and intellectual impairment [62]. By contrast, *SSBP2*, a gene involved in DNA and telomere repair and growth arrest of cancer cells [63] was also found to be upregulated in ASD LCLs.

Several miRNAs involved in cancer show dysregulated expression in ASD LCLs, including *miR-6732-3p*, *hsa-miR-221-5p* [64,65], *hsa-miR-21-5p* [66,67], *hsa-miR-152-3p* [68,69], *hsa-miR-3529-3p* [70,71], and *has-miR-148b-3p* [72,73]. Additionally, *miR-3529-3p* was 2-fold upregulated in ASD LCLs and it targets *GABRA4* (Table S7) and this miRNA promotes angiogenesis [71]. Studies have shown *miR-3529-3p* to be upregulated in radiotherapy-resistant colorectal cancer cells [70] and downregulated in liver cancer [74].

5. Conclusions

RNA-Seq analysis identified top 45 genes and 29 miRNAs that were differentially expressed in ASD LCLs compared to control LCLs. An integrated miRNA-mRNA analysis showed that the genes in significant pathways that are predicted to be targeted by

deregulated miRNAs control apoptosis, cell death of immune cells, cell cycle progression, epilepsy, and proliferation of neuronal cells. Our results reinforce findings from other groups in regard to important underlying molecular pathways and processes, such as the regulation of cell growth, the role of organs besides the brain in ASD (e.g., the immune system), and the overlap with other non-neurodevelopmental diseases, such as cancer. These findings refine the landscape of ASD genes using LCLs and show the importance of studying different cell types to understand the regulatory networks in ASD.

Supplementary Materials: The following are available online at <https://www.mdpi.com/article/10.3390/jpm12060920/s1>: Supplementary Table S1: qRT-PCR TaqMan gene expression assays for *AUTS2*, *FMR1*, *GAPDH*, and *PTEN* (ThermoFisher Scientific, Carlsbad, CA), Table S2: qRT-PCR miRNA Primer miScript Assays for *Hsa-miR-15a-5*, *Hsa-miR-92a-3p*, and *Hsa-miR-125b-5p*, *Hs_RNU6* and *Ce_miR39_1* (Qiagen, Valencia, CA). Table S3: RNA -Sequencing (RNA-Seq) analysis in LCL groups (ASD and Control). LC Sciences (Houston, TX, USA). Gene symbol, EntrezID, fold=fold change, pv = *p*-value and FDR = False discovery rate, * $p \leq 0.05$. Table S4: Small RNA -Sequencing (miRNA-Seq) analysis in LCL groups (ASD and Control), LC Sciences (Houston, TX, USA). miRNA, accession MIMATid, fold=fold change, pv = *p*-value and FDR = False discovery rate, * $p \leq 0.05$. Supplementary Table S5: Ingenuity Pathway Analysis on 1700 mRNAs (Functions and Pathways) in LCL groups (ASD and control). Supplementary Table S6: Ingenuity Pathway Analysis on 910DEGs-all miRNAs-functions-pathways in LCL groups (ASD and control). DEGs = differentially expressed genes. Supplementary Table S7: Integrated miRNA-mRNA analysis using miRWalk2.0. Ensembl, Gene, FC = Fold Change, Pathways regulated, miR = miRNA (upmiR = upregulated miRNA or downmiRs = downregulated miRNAs).

Author Contributions: Conceptualization, P.S.G. and R.E.F.; methodology, P.S.G. and H.D.; validation, S.M., K.K.V. and P.A.P.-G.; formal analysis, H.D., P.A.P.-G., P.J.W. and S.M.; data curation, H.D. and P.J.W.; writing—original draft preparation, P.S.G., P.A.P.-G., S.R. and R.E.F.; visualization, P.S.G., R.E.F. and H.D.; supervision, P.S.G. and R.E.F.; funding acquisition, R.E.F. All authors have read and agreed to the published version of the manuscript.

Funding: This research was made possible with funds from the Jonty Foundation (Saint Paul, MN, USA).

Institutional Review Board Statement: These experiments were performed on de-identified cell lines and were thus not considered human research, as verified by a determination from the University of Arkansas for Medical Sciences Investigational Review Board.

Informed Consent Statement: Not applicable.

Data Availability Statement: Data are available upon request.

Acknowledgments: We thank the families who volunteered to be involved in the research despite their demanding lives.

Conflicts of Interest: The authors declare no conflict of interest. The funders had no role in the design of the study; in the collection, analysis, or interpretation of data; in the writing of the manuscript; or in the decision to publish the results.

References

1. Maenner, M.J.; Shaw, K.A.; Bakian, A.V.; Bilder, D.A.; Durkin, M.S.; Esler, A.; Furnier, S.M.; Hallas, L.; Hall-Lande, J.; Hudson, A.; et al. Prevalence and characteristics of autism spectrum disorder among children aged 8 years—Autism and developmental disabilities monitoring network, 11 sites, United States, 2018. *MMWR Surveill. Summ.* **2021**, *70*, 1–16. [[CrossRef](#)] [[PubMed](#)]
2. Rossignol, D.A.; Frye, R.E. A review of research trends in physiological abnormalities in autism spectrum disorders: Immune dysregulation, inflammation, oxidative stress, mitochondrial dysfunction and environmental toxicant exposures. *Mol. Psychiatry* **2012**, *17*, 389–401. [[CrossRef](#)] [[PubMed](#)]
3. Al Dera, H. Cellular and molecular mechanisms underlying autism spectrum disorders and associated comorbidities: A pathophysiological review. *Biomed. Pharm.* **2022**, *148*, 112688. [[CrossRef](#)] [[PubMed](#)]
4. Frye, R.E.; Cakir, J.; Rose, S.; Palmer, R.F.; Austin, C.; Curtin, P. Physiological mediators of prenatal environmental influences in autism spectrum disorder. *Bioessays* **2021**, *43*, e2000307. [[CrossRef](#)] [[PubMed](#)]

5. Nam, H.-Y.; Shim, S.-M.; Han, B.-G.; Jeon, J.-P. Human lymphoblastoid cell lines: A goldmine for the biobankomics era. *Pharmacogenomics* **2011**, *12*, 907–917. [[CrossRef](#)]
6. Yasuda, Y.; Hashimoto, R.; Yamamori, H.; Ohi, K.; Fukumoto, M.; Umeda-Yano, S.; Mohri, I.; Ito, A.; Taniike, M.; Takeda, M. Gene expression analysis in lymphoblasts derived from patients with autism spectrum disorder. *Mol. Autism* **2011**, *2*, 9. [[CrossRef](#)]
7. Frye, R.E.; Rose, S.; McCullough, S.; Bennuri, S.C.; Porter-Gill, P.A.; Dweep, H.; Gill, P.S. MicroRNA expression profiles in autism spectrum disorder: Role for miR-181 in immunomodulation. *J. Pers. Med.* **2021**, *11*, 922. [[CrossRef](#)]
8. Bennuri, S.C.; Rose, S.; Frye, R.E. Mitochondrial dysfunction is inducible in lymphoblastoid cell lines from children with autism and may involve the TORC1 pathway. *Front. Psychiatry* **2019**, *10*, 269. [[CrossRef](#)]
9. James, S.J.; Rose, S.; Melnyk, S.; Jernigan, S.; Blossom, S.; Pavliv, O.; Gaylor, D.W. Cellular and mitochondrial glutathione redox imbalance in lymphoblastoid cells derived from children with autism. *FASEB J.* **2009**, *23*, 2374–2383. [[CrossRef](#)]
10. Rose, S.; Bennuri, S.C.; Wynne, R.; Melnyk, S.; James, S.J.; Frye, R.E. Mitochondrial and redox abnormalities in autism lymphoblastoid cells: A sibling control study. *FASEB J.* **2017**, *31*, 904–909. [[CrossRef](#)]
11. Saeli, T.; Tangsuwansri, C.; Thongkorn, S.; Chonchaiya, W.; Suphapeetiporn, K.; Mutirangura, A.; Tencomnao, T.; Hu, V.; Sarachana, T. Integrated genome-wide Alu methylation and transcriptome profiling analyses reveal novel epigenetic regulatory networks associated with autism spectrum disorder. *Mol. Autism* **2018**, *9*, 27. [[CrossRef](#)] [[PubMed](#)]
12. Frye, R.E.; Nankova, B.; Bhattacharyya, S.; Rose, S.; Bennuri, S.C.; MacFabe, D.F. Modulation of immunological pathways in autistic and neurotypical lymphoblastoid cell lines by the enteric microbiome metabolite propionic acid. *Front. Immunol.* **2017**, *8*, 1670. [[CrossRef](#)]
13. Ambros, V. The functions of animal microRNAs. *Nature* **2004**, *431*, 350–355. [[CrossRef](#)] [[PubMed](#)]
14. Sarachana, T.; Zhou, R.; Chen, G.; Manji, H.K.; Hu, V.W. Investigation of post-transcriptional gene regulatory networks associated with autism spectrum disorders by microRNA expression profiling of lymphoblastoid cell lines. *Genome Med.* **2010**, *2*, 23. [[CrossRef](#)] [[PubMed](#)]
15. Talebizadeh, Z.; Butler, M.G.; Theodoro, M.F. Feasibility and relevance of examining lymphoblastoid cell lines to study role of microRNAs in autism. *Autism Res.* **2008**, *1*, 240–250. [[CrossRef](#)]
16. Langmead, B.; Trapnell, C.; Pop, M.; Salzberg, S.L. Ultrafast and memory-efficient alignment of short DNA sequences to the human genome. *Genome Biol.* **2009**, *10*, R25. [[CrossRef](#)]
17. Li, B.; Dewey, C.N. RSEM: Accurate transcript quantification from RNA-Seq data with or without a reference genome. *BMC Bioinformatics* **2011**, *12*, 323. [[CrossRef](#)]
18. Love, M.I.; Huber, W.; Anders, S. Moderated estimation of fold change and dispersion for RNA-seq data with DESeq2. *Genome Biol.* **2014**, *15*, 550. [[CrossRef](#)]
19. Dweep, H.; Sticht, C.; Pandey, P.; Gretz, N. miRWalk–database: Prediction of possible miRNA binding sites by “walking” the genes of three genomes. *J. Biomed. Inf.* **2011**, *44*, 839–847. [[CrossRef](#)]
20. Dweep, H.; Gretz, N. miRWalk2.0: A comprehensive atlas of microRNA-target interactions. *Nat. Methods* **2015**, *12*, 697. [[CrossRef](#)]
21. Dweep, H.; Gretz, N.; Felekis, K. A schematic workflow for collecting information about the interaction between copy number variants and microRNAs using existing resources. *Methods Mol. Biol.* **2014**, *1182*, 307–320. [[PubMed](#)]
22. Papagregoriou, G.; Erguler, K.; Dweep, H.; Voskarides, K.; Koupepidou, P.; Athanasiou, Y.; Pierides, A.; Gretz, N.; Felekis, K.N.; Deltas, C.A. A miR-1207-5p binding site polymorphism abolishes regulation of HBEGF and is associated with disease severity in CFHR5 nephropathy. *PLoS ONE* **2012**, *7*, e31021. [[CrossRef](#)] [[PubMed](#)]
23. Frye, R.E.; Rose, S.; McCullough, S.; Bennuri, S.C.; Porter-Gill, P.A.; Dweep, H.; Gill, P.S. miRNA expression profiles in autism spectrum disorders. *Brain Res.* **2011**, *1380*, 922.
24. Talebizadeh, Z.; Aldenderfer, R.; Chen, X.W. A proof-of-concept study: Exon-level expression profiling and alternative splicing in autism using lymphoblastoid cell lines. *Psychiatr. Genet.* **2014**, *24*, 1–9. [[CrossRef](#)]
25. Hu, V.W.; Sarachana, T.; Kim, K.S.; Nguyen, A.; Kulkarni, S.; Steinberg, M.E.; Luu, T.; Lai, Y.; Lee, N.H. Gene expression profiling differentiates autism case-controls and phenotypic variants of autism spectrum disorders: Evidence for circadian rhythm dysfunction in severe autism. *Autism Res.* **2009**, *2*, 78–97. [[CrossRef](#)]
26. Nishimura, Y.; Martin, C.L.; Vazquez-Lopez, A.; Spence, S.J.; Alvarez-Retuerto, A.I.; Sigman, M.; Steindler, C.; Pellegrini, S.; Schanen, N.C.; Warren, S.T.; et al. Genome-wide expression profiling of lymphoblastoid cell lines distinguishes different forms of autism and reveals shared pathways. *Hum. Mol. Genet.* **2007**, *16*, 1682–1698. [[CrossRef](#)]
27. Ma, D.Q.; Whitehead, P.L.; Menold, M.M.; Martin, E.R.; Ashley-Koch, A.E.; Mei, H.; Ritchie, M.D.; Delong, G.R.; Abramson, R.K.; Wright, H.H.; et al. Identification of significant association and gene-gene interaction of GABA receptor subunit genes in autism. *Am. J. Hum. Genet.* **2005**, *77*, 377–388. [[CrossRef](#)]
28. Griswold, A.J.; Van Booven, D.; Cuccaro, M.L.; Haines, J.L.; Gilbert, J.R.; Pericak-Vance, M.A. Identification of rare noncoding sequence variants in gamma-aminobutyric acid A receptor, alpha 4 subunit in autism spectrum disorder. *Neurogenetics* **2018**, *19*, 17–26. [[CrossRef](#)]
29. Chandra, D.; Jia, F.; Liang, J.; Peng, Z.; Suryanarayanan, A.; Werner, D.F.; Spigelman, I.; Houser, C.R.; Olsen, R.W.; Harrison, N.L.; et al. GABAA receptor alpha 4 subunits mediate extrasynaptic inhibition in thalamus and dentate gyrus and the action of gaboxadol. *Proc. Natl. Acad. Sci. USA* **2006**, *103*, 15230–15235. [[CrossRef](#)]

30. Beunders, G.; de Munnik, S.A.; Van der Aa, N.; Ceulemans, B.; Voorhoeve, E.; Groffen, A.J.; Nillesen, W.M.; Meijers-Heijboer, E.J.; Kooy, R.F.; Yntema, H.G.; et al. Two male adults with pathogenic AUTS2 variants, including a two-base pair deletion, further delineate the AUTS2 syndrome. *Eur. J. Hum. Genet.* **2015**, *23*, 803–807. [[CrossRef](#)]
31. Beunders, G.; van de Kamp, J.; Vasudevan, P.; Morton, J.; Smets, K.; Kleefstra, T.; de Munnik, S.A.; Schuurs-Hoeijmakers, J.; Ceulemans, B.; Zollino, M.; et al. A detailed clinical analysis of 13 patients with AUTS2 syndrome further delineates the phenotypic spectrum and underscores the behavioural phenotype. *J. Med. Genet.* **2016**, *53*, 523–532. [[CrossRef](#)]
32. Beunders, G.; Voorhoeve, E.; Golzio, C.; Pardo, L.M.; Rosenfeld, J.A.; Talkowski, M.E.; Simonic, I.; Lionel, A.C.; Vergult, S.; Pyatt, R.E.; et al. Exonic deletions in AUTS2 cause a syndromic form of intellectual disability and suggest a critical role for the C terminus. *Am. J. Hum. Genet.* **2013**, *92*, 210–220. [[CrossRef](#)] [[PubMed](#)]
33. Sanchez-Jimeno, C.; Blanco-Kelly, F.; López-Grondona, F.; Losada-Del Pozo, R.; Moreno, B.; Rodrigo-Moreno, M.; Martinez-Cayuelas, E.; Riveiro-Alvarez, R.; Fenollar-Cortés, M.; Ayuso, C.; et al. Attention deficit hyperactivity and autism spectrum disorders as the core symptoms of AUTS2 syndrome: Description of five new patients and update of the frequency of manifestations and genotype-phenotype correlation. *Genes* **2021**, *12*, 1360. [[CrossRef](#)] [[PubMed](#)]
34. Rossignol, D.A.; Frye, R.E. A systematic review and meta-analysis of immunoglobulin g abnormalities and the therapeutic use of intravenous immunoglobulins (IVIG) in autism spectrum disorder. *J. Pers. Med.* **2021**, *11*, 488. [[CrossRef](#)] [[PubMed](#)]
35. Heuer, L.; Ashwood, P.; Schauer, J.; Goines, P.; Krakowiak, P.; Hertz-Picciotto, I.; Hansen, R.; Croen, L.A.; Pessah, I.N.; Van de Water, J. Reduced levels of immunoglobulin in children with autism correlates with behavioral symptoms. *Autism Res.* **2008**, *1*, 275–283. [[CrossRef](#)] [[PubMed](#)]
36. Nortey, A.N.; Garces, K.N.; Hackam, A.S. Exploring the role of interleukin-27 as a regulator of neuronal survival in central nervous system diseases. *Neural Regen. Res.* **2022**, *17*, 2149–2152.
37. Ahmad, S.F.; Ansari, M.A.; Nadeem, A.; Bakheet, S.A.; Al-Ayadhi, L.Y.; Attia, S.M. Toll-like receptors, NF- κ B, and IL-27 mediate adenosine A2A receptor signaling in BTBR T(+) Itr3(tf)/J mice. *Prog. Neuropsychopharmacol. Biol. Psychiatry* **2017**, *79*, 184–191. [[CrossRef](#)]
38. Ahmad, S.F.; Bakheet, S.A.; Ansari, M.A.; Nadeem, A.; Alobaidi, A.F.; Attia, S.M.; Alhamed, A.S.; Aldossari, A.A.; Mahmoud, M.A. Methylmercury chloride exposure aggravates proinflammatory mediators and Notch-1 signaling in CD14(+) and CD40(+) cells and is associated with imbalance of neuroimmune function in BTBR T(+) Itr3tf/J mice. *Neurotoxicology* **2021**, *82*, 9–17. [[CrossRef](#)]
39. Ahmad, S.F.; Ansari, M.A.; Nadeem, A.; Bakheet, S.A.; Alsanea, S.; Al-Hosaini, K.A.; Mahmood, H.M.; Alzahrani, M.Z.; Attia, S.M. Inhibition of tyrosine kinase signaling by tyrphostin AG126 downregulates the IL-21/IL-21R and JAK/STAT pathway in the BTBR mouse model of autism. *Neurotoxicology* **2020**, *77*, 1–11. [[CrossRef](#)]
40. Ahmad, S.F.; Nadeem, A.; Ansari, M.A.; Bakheet, S.A.; Attia, S.M.; Zoheir, K.M.; Al-Ayadhi, L.Y.; Alzahrani, M.Z.; Alsaad, A.M.; Alotaibi, M.R.; et al. Imbalance between the anti- and pro-inflammatory milieu in blood leukocytes of autistic children. *Mol. Immunol.* **2017**, *82*, 57–65. [[CrossRef](#)]
41. Song, Z.; Han, X.; Shen, L.; Zou, H.; Zhang, B.; Liu, J.; Gong, A. PTEN silencing enhances neuronal proliferation and differentiation by activating PI3K/Akt/GSK3 β pathway in vitro. *Exp. Cell Res.* **2018**, *363*, 179–187. [[CrossRef](#)] [[PubMed](#)]
42. Fan, C.; Gao, Y.; Liang, G.; Huang, L.; Wang, J.; Yang, X.; Shi, Y.; Dräger, U.C.; Zhong, M.; Gao, T.M.; et al. Transcriptomics of Gabra4 knockout mice reveals common NMDAR pathways underlying autism, memory, and epilepsy. *Mol. Autism* **2020**, *11*, 13. [[CrossRef](#)]
43. Roberts, D.S.; Raol, Y.H.; Bandyopadhyay, S.; Lund, I.V.; Budreck, E.C.; Passini, M.A.; Wolfe, J.H.; Brooks-Kayal, A.R.; Russek, S.J. Egr3 stimulation of GABRA4 promoter activity as a mechanism for seizure-induced up-regulation of GABA(A) receptor alpha4 subunit expression. *Proc. Natl. Acad. Sci. USA* **2005**, *102*, 11894–11899. [[CrossRef](#)] [[PubMed](#)]
44. Caracci, M.O.; Avila, M.E.; Espinoza-Cavieres, F.A.; López, H.R.; Ugarte, G.D.; De Ferrari, G.V. Wnt/ β -Catenin-dependent transcription in autism spectrum disorders. *Front. Mol. Neurosci.* **2021**, *14*, 764756. [[CrossRef](#)] [[PubMed](#)]
45. Platt, R.J.; Zhou, Y.; Slaymaker, I.M.; Shetty, A.S.; Weisbach, N.R.; Kim, J.A.; Sharma, J.; Desai, M.; Sood, S.; Kempton, H.R.; et al. Chd8 mutation leads to autistic-like behaviors and impaired striatal circuits. *Cell Rep.* **2017**, *19*, 335–350. [[CrossRef](#)] [[PubMed](#)]
46. Marcogliese, P.C.; Dutta, D.; Ray, S.S.; Dang, N.D.P.; Zuo, Z.; Wang, Y.; Lu, D.; Fazal, F.; Ravenscroft, T.A.; Chung, H.; et al. Loss of IRF2BPL impairs neuronal maintenance through excess Wnt signaling. *Sci. Adv.* **2022**, *8*, eabl5613. [[CrossRef](#)]
47. Liu, X.; Hu, G.; Ye, J.; Ye, B.; Shen, N.; Tao, Y.; Zhang, X.; Fan, Y.; Liu, H.; Zhang, Z.; et al. De Novo ARID1B mutations cause growth delay associated with aberrant Wnt/ β -catenin signaling. *Hum. Mutat.* **2020**, *41*, 1012–1024. [[CrossRef](#)]
48. Crawley, J.N.; Heyer, W.D.; LaSalle, J.M. Autism and cancer share risk genes, pathways, and drug targets. *Trends Genet.* **2016**, *32*, 139–146. [[CrossRef](#)]
49. Sumia, I.; Pierani, A.; Causeret, F. Kremen1-induced cell death is regulated by homo- and heterodimerization. *Cell Death Discov.* **2019**, *5*, 91. [[CrossRef](#)]
50. Cheng, J.; Li, M.; Tzeng, C.M.; Gou, X.; Chen, S. Suppression of tumorigenicity 5 ameliorates tumor characteristics of invasive breast cancer cells via ERK/JNK pathway. *Front. Oncol.* **2021**, *11*, 621500. [[CrossRef](#)]
51. Emami, N.C.; Cavazos, T.B.; Rashkin, S.R.; Cario, C.L.; Graff, R.E.; Tai, C.G.; Mefford, J.A.; Kachuri, L.; Wan, E.; Wong, S.; et al. A large-scale association study detects novel rare variants, risk genes, functional elements, and polygenic architecture of prostate cancer susceptibility. *Cancer Res.* **2021**, *81*, 1695–1703. [[CrossRef](#)] [[PubMed](#)]
52. Kim, J.-H.; Hwang, J.; Jung, J.H.; Lee, H.-J.; Lee, D.Y.; Kim, S.-H. Molecular networks of FOXP family: Dual biologic functions, interplay with other molecules and clinical implications in cancer progression. *Mol. Cancer* **2019**, *18*, 180. [[CrossRef](#)] [[PubMed](#)]

53. Bartaula-Brevik, S.; Brattås, M.K.L.; Tvedt, T.; Reikvam, H.; Bruserud, Ø. Splenic tyrosine kinase (SYK) inhibitors and their possible use in acute myeloid leukemia. *Expert Opin. Investig. Drugs* **2018**, *27*, 377–387. [[CrossRef](#)]
54. Kanegasaki, S.; Tsuchiya, T. A possible way to prevent the progression of bone lesions in multiple myeloma via Src-homology-region-2-domain-containing-phosphatase-1 activation. *J. Cell Biochem.* **2021**, *122*, 1313–1325. [[CrossRef](#)]
55. Profitós-Pelejà, N.; Santos, J.C.; Marín-Niebla, A.; Roué, G.; Ribeiro, M.L. Regulation of B-cell receptor signaling and its therapeutic relevance in aggressive B-cell lymphomas. *Cancers* **2022**, *14*, 860. [[CrossRef](#)] [[PubMed](#)]
56. Chen, W.; Xu, Y.; Zhong, J.; Wang, H.; Weng, M.; Cheng, Q.; Wu, Q.; Sun, Z.; Jiang, H.; Zhu, M.; et al. MFHAS1 promotes colorectal cancer progress by regulating polarization of tumor-associated macrophages via STAT6 signaling pathway. *Oncotarget* **2016**, *7*, 78726–78735. [[CrossRef](#)]
57. Yang, S.; Jeung, H.-C.; Jeong, H.J.; Choi, Y.H.; Kim, J.E.; Jung, J.-J.; Rha, S.Y.; Yang, W.I.; Chung, H.C. Identification of genes with correlated patterns of variations in DNA copy number and gene expression level in gastric cancer. *Genomics* **2007**, *89*, 451–459. [[CrossRef](#)]
58. Mareschal, S.; Dubois, S.; Viailly, P.J.; Bertrand, P.; Bohers, E.; Maingonnat, C.; Jaïs, J.P.; Tesson, B.; Ruminy, P.; Peyrouze, P.; et al. Whole exome sequencing of relapsed/refractory patients expands the repertoire of somatic mutations in diffuse large B-cell lymphoma. *Genes Chromosomes Cancer* **2016**, *55*, 251–267. [[CrossRef](#)]
59. Kang, J. Genomic alterations on 8p21-p23 are the most frequent genetic events in stage I squamous cell carcinoma of the lung. *Exp. Ther. Med.* **2015**, *9*, 345–350. [[CrossRef](#)]
60. Stachelscheid, J.; Jiang, Q.; Herling, M. The modes of dysregulation of the proto-oncogene T-cell leukemia/lymphoma 1A. *Cancers* **2021**, *13*, 5455. [[CrossRef](#)]
61. Zhong, J.; Guo, C.; Hou, W.; Shen, N.; Miao, C. Effects of MFHAS1 on cognitive impairment and dendritic pathology in the hippocampus of septic rats. *Life Sci.* **2019**, *235*, 116822. [[CrossRef](#)]
62. Choucair, N.; Rajab, M.; Mégarbané, A.; Chouery, E. Homozygous microdeletion of the ERI1 and MFHAS1 genes in a patient with intellectual disability, limb abnormalities, and cardiac malformation. *Am. J. Med. Genet. A* **2017**, *173*, 1955–1960. [[CrossRef](#)]
63. Chung, Y.; Kim, H.; Bang, S.; Jang, K.; Paik, S.S.; Shin, S.J. Nuclear expression loss of SSBP2 is associated with poor prognostic factors in colorectal adenocarcinoma. *Diagnostics* **2020**, *10*, 1097. [[CrossRef](#)] [[PubMed](#)]
64. Ye, J.; Xu, W.; Chen, T. Identification of onco-miRNAs in hepatocellular carcinoma and analysis of their regulatory network. *Nan Fang Yi Ke Da Xue Xue Bao* **2022**, *42*, 45–54.
65. Leidinger, P.; Hart, M.; Backes, C.; Rheinheimer, S.; Keck, B.; Wullich, B.; Keller, A.; Meese, E. Differential blood-based diagnosis between benign prostatic hyperplasia and prostate cancer: miRNA as source for biomarkers independent of PSA level, Gleason score, or TNM status. *Tumour Biol.* **2016**, *37*, 10177–10185. [[CrossRef](#)]
66. Sequeira, J.P.; Constâncio, V.; Salta, S.; Lobo, J.; Barros-Silva, D.; Carvalho-Maia, C.; Rodrigues, J.; Braga, I.; Henrique, R.; Jerónimo, C. LiKidMiRs: A ddPCR-based panel of 4 circulating miRNAs for detection of renal cell carcinoma. *Cancers* **2022**, *14*, 858. [[CrossRef](#)] [[PubMed](#)]
67. Farré, P.L.; Duca, R.B.; Massillo, C.; Dalton, G.N.; Graña, K.D.; Gardner, K.; Lacunza, E.; De Siervi, A. MiR-106b-5p: A master regulator of potential biomarkers for breast cancer aggressiveness and prognosis. *Int. J. Mol. Sci.* **2021**, *22*, 11135. [[CrossRef](#)] [[PubMed](#)]
68. Kang, Y.Y.; Liu, Y.; Wang, M.L.; Guo, M.; Wang, Y.; Cheng, Z.F. Construction and analyses of the microRNA-target gene differential regulatory network in thyroid carcinoma. *PLoS ONE* **2017**, *12*, e0178331. [[CrossRef](#)]
69. Ge, S.; Wang, D.; Kong, Q.; Gao, W.; Sun, J. Function of miR-152 as a tumor suppressor in human breast cancer by targeting PIK3CA. *Oncol Res.* **2017**, *25*, 1363–1371. [[CrossRef](#)]
70. Shang, Y.; Wang, L.; Zhu, Z.; Gao, W.; Li, D.; Zhou, Z.; Chen, L.; Fu, C.G. Downregulation of miR-423-5p contributes to the radioresistance in colorectal cancer cells. *Front. Oncol.* **2020**, *10*, 582239. [[CrossRef](#)]
71. Kinget, L.; Roussel, E.; Verbiest, A.; Albersen, M.; Rodríguez-Antona, C.; Graña-Castro, O.; Inglada-Pérez, L.; Zucman-Rossi, J.; Couchy, G.; Job, S.; et al. MicroRNAs targeting HIF-2 α , VEGFR1 and/or VEGFR2 as potential predictive biomarkers for VEGFR tyrosine kinase and HIF-2 α inhibitors in metastatic clear-cell renal cell carcinoma. *Cancers* **2021**, *13*, 3099. [[CrossRef](#)]
72. Liu, G.; Mao, H.; Liu, Y.; Zhang, Z.; Ha, S.; Zhang, X. miR-148b-3p, as a tumor suppressor, targets son of sevenless homolog 1 to regulate the malignant progression in human osteosarcoma. *Bioengineered* **2022**, *13*, 4271–4284. [[CrossRef](#)] [[PubMed](#)]
73. Jiang, X.; Jing, Y.; Lei, L.; Peng, M.; Xiao, Q.; Ren, J.; Tao, Y.; Huang, J.; Zhang, L. miR-148b-3p inhibits the proliferation and autophagy of acute myeloid leukemia cells by targeting ATG14. *Xi Bao Yu Fen Zi Mian Yi Xue Za Zhi* **2021**, *37*, 881–890. [[PubMed](#)]
74. Weng, Z.; Peng, J.; Wu, W.; Zhang, C.; Zhao, J.; Gao, H. Downregulation of PART1 inhibits proliferation and differentiation of Hep3B cells by targeting hsa-miR-3529-3p/FOXC2 Axis. *J. Oncol.* **2021**, *2021*, 7792223. [[CrossRef](#)] [[PubMed](#)]